catalysts

MDPI

Article

Dehydrogenation of Formic Acid over a Homogeneous Ru-TPPTS Catalyst: Unwanted CO Production and Its Successful Removal by PROX

Vera Henricks [1,2], Igor Yuranov [3], Nordahl Autissier [3] and Gábor Laurenczy [1,*]

[1] Laboratory of Organometallic and Medical Chemistry, Group of Catalysis for Energy and Environment, École Polytechnique Fédérale de Lausanne, EPFL, CH-1015 Lausanne, Switzerland; v.c.henricks@student.tue.nl
[2] Molecular Catalysis, Department of Chemical Engineering and Chemistry, Eindhoven University of Technology, 5612 AZ Eindhoven, The Netherlands
[3] GRT Operations SA, CH-1350 Orbe, Switzerland; igor.iouranov@gmail.com (I.Y.); nordahl.autissier@grtgroup.swiss (N.A.)
* Correspondence: gabor.laurenczy@epfl.ch; Tel.: +41-21-693-9858

Received: 26 October 2017; Accepted: 13 November 2017; Published: 20 November 2017

Abstract: Formic acid (FA) is considered as a potential durable energy carrier. It contains ~4.4 wt % of hydrogen (or 53 g/L) which can be catalytically released and converted to electricity using a proton exchange membrane (PEM) fuel cell. Although various catalysts have been reported to be very selective towards FA dehydrogenation (resulting in H_2 and CO_2), a side-production of CO and H_2O (FA dehydration) should also be considered, because most PEM hydrogen fuel cells are poisoned by CO. In this research, a highly active aqueous catalytic system containing Ru(III) chloride and meta-trisulfonated triphenylphosphine (*m*TPPTS) as a ligand was applied for FA dehydrogenation in a continuous mode. CO concentration (8–70 ppm) in the resulting $H_2 + CO_2$ gas stream was measured using a wide range of reactor operating conditions. The CO concentration was found to be independent on the reactor temperature but increased with increasing FA feed. It was concluded that unwanted CO concentration in the $H_2 + CO_2$ gas stream was dependent on the current FA concentration in the reactor which was in turn dependent on the reaction design. Next, preferential oxidation (PROX) on a Pt/Al_2O_3 catalyst was applied to remove CO traces from the $H_2 + CO_2$ stream. It was demonstrated that CO concentration in the stream could be reduced to a level tolerable for PEM fuel cells (~3 ppm).

Keywords: formic acid; dehydrogenation; dehydration; ruthenium; carbon monoxide; preferential oxidation; PROX

---

1. Introduction

Currently, many methods to store and/or to transport energy in a green and durable way are being investigated in order to transition to an environmentally friendly economy. Examples include mechanical storage, batteries, superconductors, chemical storage (hydrogen and other high energy molecules) [1,2]. Formic acid (FA) containing ~4.4 wt % of H_2 has been considered a potential energy carrier since 1978 [3]. Essentially, H_2 could be chemically combined with carbon dioxide (CO_2) to form liquid FA [4], which is more easily stored and transported than gaseous H_2 considering practical and safety issues. FA can then be catalytically decomposed back to H_2 and CO_2 in a 1:1 ratio, closing a loop for CO_2 and providing H_2 for fuel cell technology to generate electricity. Thus, FA would simply function as an intermediate to store and to transport energy in a clean way (Figure 1).

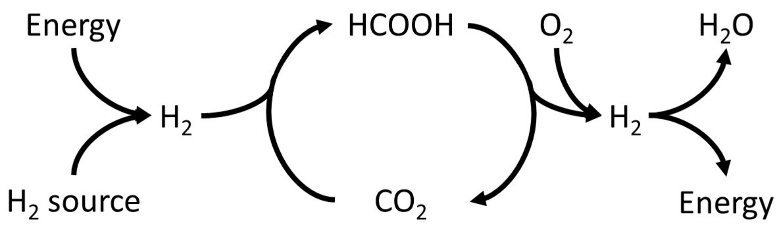

Figure 1. Formic acid as an energy carrier providing a closed loop for CO_2.

Recently, FA has sparked interest again, because catalysts highly effective in FA dehydrogenation in reasonable conditions have been found [5–9]. This fact in combination with easy and safe handling opens a route of using FA in applications such as energy storage and transport [10].

Although very high catalyst selectivities have been reported in literature [7,9,11], a side-reaction of FA dehydration takes usually place, next to FA dehydrogenation, due to a still insufficient catalyst selectivity and/or thermal decomposition of FA:

$$HCOOH \rightarrow H_2 + CO_2, \tag{1}$$

$$HCOOH \rightarrow H_2O + CO. \tag{2}$$

It is very important to consider this side-reaction, because a CO content, even at ppm-levels, is poisonous for many fuel cells [12,13]. FA thermal decomposition was investigated both computationally and experimentally. However, most of the experiments were conducted in supercritical water [14–17].

Mitigating strategies such as improving CO-tolerance of fuel cells showed that Pt–Ru alloying, for example, can weaken the binding of CO to Pt catalysts, decreasing the poisoning effect [18,19]. Air-bleed—injecting a small amount of air or oxygen into the fuel feed stream—is also applied to lessen CO poisoning. Here, CO oxidation takes place directly on a fuel cell membrane as an oxidation catalyst. The method can recover up to 90% of the fuel cell performance at 200 ppm CO [20,21]. However, air-bleed was shown to cause long-term degradation of the membrane where O_2 is reduced to H_2O_2 which corrodes the catalyst [22]. To avoid this problem, preferential oxidation (PROX) could be used to decrease CO concentration. In this approach, CO is removed from the H_2 stream through injecting a small amount of O_2 and selective CO oxidation over a heterogeneous catalyst prior to entering the fuel cell. Nowadays, PROX is mainly applied to bulk production of H_2 where a significant CO amount (0.5–1%) is produced through steam reforming and water gas shift reactions [23]. Several catalysts such as noble metals supported on alumina or ceria as well as transition metals on similar supports are available [24]. The catalysts are designed to work in gas streams containing at least 85% of H_2. In H_2 rich gas streams, Equations (3) and (4) are of importance

$$2CO + O_2 \rightarrow 2CO_2 \tag{3}$$

$$2H_2 + O_2 \rightarrow 2H_2O \tag{4}$$

To minimize H_2 loss and H_2O emittance (Equation (4)), the catalyst selectivity towards CO oxidation needs to be as high as possible. An important factor is the amount of supplied O_2, because selective catalysts start converting H_2 after complete CO conversion [24]. Moreover, FA dehydrogenation gas mixtures contain much more CO_2 (~50%) which could possibly effect the conversion of CO.

Other methods to remove CO from gas streams are adsorption and methanation. However, it is hard to implement pressure swing CO adsorption in compact applications [25]. Methanation is usually mentioned as an option next to PROX:

$$CO + 3H_2 \rightarrow CH_4 + H_2O, \tag{5}$$

$$CO_2 + 4H_2 \rightarrow CH_4 + 2H_2O. \tag{6}$$

Supported Ni and Ru methanation catalysts are well investigated [26]. Fuel cells are tolerant to methane [12]. No gas needs to be added to the stream. However, significant amount of H_2 could be lost in this process depending on the CO concentration and catalyst selectivity towards CO methanation. Next to that, most of the methanation catalysts become active only at temperatures over 250 °C.

In the present study, a H_2 + CO_2 gas mixture (reformate) resulted from catalytic FA dehydrogenation carried out in a continuous-flow gas–liquid bed reactor was analyzed. The liquid reaction phase was comprised of an aqueous solution of Ru(III) chloride and *m*TPPTS used as catalyst precursors. *m*TPPTS was chosen as a phosphine-ligand because of its high stability and water solubility of the resulting catalytically active complex [7]. Previously, it was reported that this catalyst was stable over more than one year of intermittent use, while being kept in air [27]. The turnover frequencies (TOF's) reached in a continuous mode were 210 h^{-1} and 670 h^{-1} at 100 °C and 120 °C, respectively [27]. CO content in the resulting gas mixture was not measured in a continuous mode, but batch experiments performed using the same reactant concentrations showed no CO traces (detection limit ~3 ppm) [7].

In the present study, FA was fed to the reactor continuously. The CO concentration (ppm level) in the H_2 + CO_2 gas streams was measured as a function of the reaction temperature and FA feed flow. Quantification of such low CO concentrations (especially in CO_2-rich gas mixtures) is an extremely difficult task. In this research, gas chromatography (GC) coupled with sample methanation was used to achieve a good CO/CO_2 separation and sensibility of the measurements, while it was also possible to measure a H_2 concentration.

Next, CO removal from H_2 + CO_2 gas streams by PROX was tested using a commercially available Pt/Al_2O_3 catalyst placed downstream from the FA dehydrogenation reactor. The PROX catalyst was not heated. A controlled amount of O_2 (in air) was injected into the gas stream before the PROX catalyst. The considered parameters were the CO concentration in the gas stream and the amount of added O_2. A combination of these numbers can be expressed through the O_2 excess parameter λ (Equation (7)), representing the O_2 excess, relatively to its amount required for total CO oxidation. At $\lambda = 1$, the O_2 concentration in a gas mixture is exactly enough to convert all CO (catalyst selectivity ~100%)

$$\lambda = \frac{2C_{O_2}}{C_{CO}} = \frac{2p_{O_2}}{p_{CO}} \tag{7}$$

2. Results and Discussion

2.1. CO *Side-Production in FA Dehydrogenation*

The CO concentration in H_2 + CO_2 gas mixtures was measured in the reaction temperature range of 60–80 °C. Below 60 °C, the Pt/Al_2O_3 catalyst activity was too low for the application, while at 80 °C and higher, water evaporation became quite intensive constantly reducing the catalyst solution volume. At a steady-state, the total gas flow rate was found to be the same for the all measured temperatures (Table 1) indicating that in this temperature range the reaction rate was limited by the FA feed flow rate.

Table 1. Total $H_2 + CO_2$ gas flow as a function of FA feed measured at 60, 70 and 80 °C.

FA Feed (mL/min)	Total Gas Flow (L/min)
0.3	0.43
0.6	0.86
0.9	1.29

As can be seen in Figure 2, the CO concentration in the gas mixture was below 10 ppm at the FA feed flow rate of 0.3 mL/min but increased with increasing FA feed. It was supposed that, due to an imperfect reactant mixing in the reactor, at the high FA feed flow rates the size of injected FA droplets is bigger and hence their lifetime is longer. At higher temperatures, it leads to more pronounced side-reaction of FA thermal dehydration and higher CO content in the reformate.

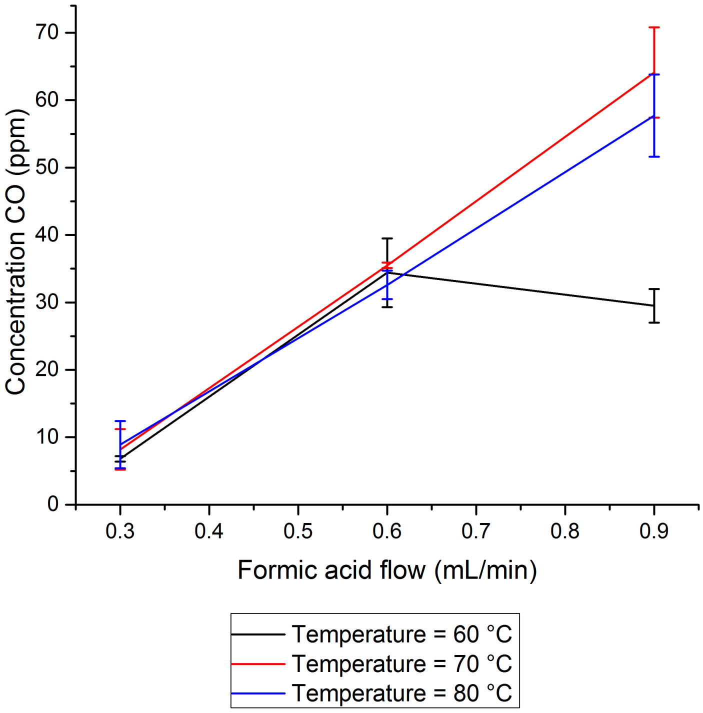

Figure 2. CO concentration in $H_2 + CO_2$ gas mixtures as a function of FA feed flow and temperature.

2.2. PROX

Figure 3 shows CO concentrations in $H_2 + CO_2$ gas mixtures treated on the PROX catalyst. Varying the FA feed flow at constant reaction temperature, both the total gas flow rate and CO concentration were varied. It was observed during the experiments that the catalyst container became warm (50–60 °C) due to the exothermic oxidation of CO and H_2. It was found for all reformate flow rates that at high concentrations of injected O_2 (λ = 3–14), the PROX treatment led to a drop in the CO concentrations to ~3 ppm. At λ = 1–2 a small increase of the resulting CO concentration up to 4–6 ppm was observed. Surprisingly, at $\lambda < 1$, a high CO conversion was observed as well (Figure 3). This fact was explained by the presence of a considerable amount of O_2 adsorbed on the catalyst surface. After an N_2 purge of the PROX catalyst for three days, the CO concentration decreased under the same conditions ($\lambda < 1$) from initial 35 to 16 ppm indicating O_2 strongly adsorbed on the catalyst that could not be removed by a simple purge.

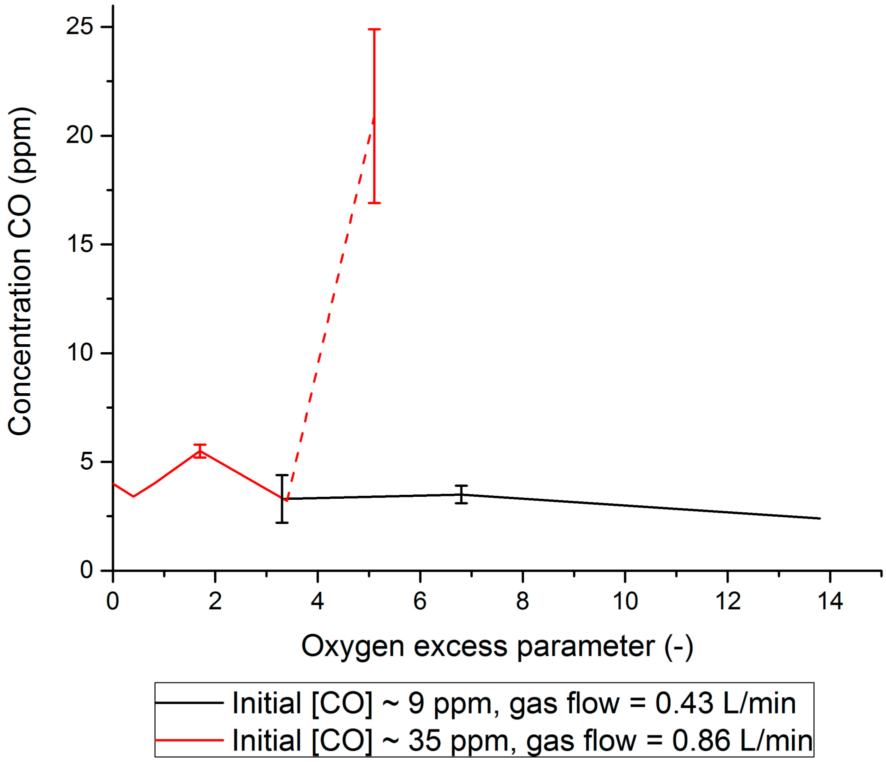

Figure 3. CO concentration after PROX oxidation in $H_2 + CO_2$ gas mixtures as a function of initial CO concentration, total flow rate, and injected O_2.

It is worth noticing that at the total $H_2 + CO_2$ gas flow rate of 0.86 L/min and high O_2 concentrations ($\lambda > 5$), water condensation in the PROX catalyst container and drop of the CO conversion were detected (Figure 3) indicating a blockage of the catalyst surface by water.

This effect was previously reported for PROX catalysts [24]. For the lower gas flow rates, water clogging was observed only after a long period of catalyst exposure. The activity of the catalyst deactivated by the water clogging could be completely recovered by an air or nitrogen purge at room temperature.

3. Materials and Methods

A homogeneous Ru-*m*TPPTS catalyst (*m*TPPTS: meta-trisulfonated triphenylphosphine, Figure 4) solution (33 mM, 700 mL) was prepared by combining an aqueous solution of $RuCl_3$ (5.6 g) and *m*TPPTS (2.8 equivalent) with FA (128 g) and Na formate (30 g). The catalyst was activated prior to its placing into the reactor by steering the solution at 60 °C for 4 h under a N_2 flow.

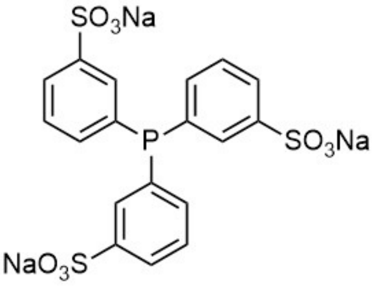

Figure 4. TPPTS.

FA was dehydrogenated in a 1 L continuous-flow gas–liquid bed reactor (Figure 5). A cylindrical, non-stirred reactor vessel of a 7.0 cm inner diameter and 40 cm length was heated by means of an internal heating element connecting to an oil circulator (Huber Pilot One). The temperature inside the reactor was varied in the range of 60–80 °C. FA was injected into the reactor (0.3–0.9 mL/min) at the reactor bottom through a HPLC pump (HPLC Pump 422, Kontron Instruments, Montigny Le Bretonneux, France). The gas bubbles produced due to the reaction rose, mixing the reaction solution. Outside the reactor, a $H_2 + CO_2$ gas mixture was passed through a condenser and an adsorber (activated carbon) to remove FA and water vapors. The total gas flow was measured using a bubble flowmeter. In separate experiments, a $H_2 + CO_2$ gas mixture was passed through a container of 2.8 cm inner diameter, containing a PROX catalyst (50 g). A commercial 0.5 wt % Pt supported on alumina (spheres of 1.8–3.5 mm diameter, Johnson Matthey, Royston, UK) was used as a PROX catalyst. An air flow controlled by a mass flow controller was injected into the gas stream before the PROX catalyst.

Gas samples were collected at a steady state before and after the PROX catalyst using a rubber balloon flushed with nitrogen and vacuumed. The collected gas samples were analyzed by a GC method using an Agilent 7890B gas chromatograph (Agilent, Santa Clara, CA, USA) equipped with a CarboPlot P7 column (25 m × 0.53 mm × 25 µm), a Nickel Catalyst Kit (to convert CO (CO_2) to CH_4), flame ionization (FID), and thermal conductivity (TCD) detectors. At least three samples were taken for every point. At least three GC measurements were done for every gas sample. The GC was calibrated using standard (50% H_2 + 40 ppm CO + CO_2) and (50% CO_2 + 100 ppm CO + N_2) mixtures (Carbagas, Lausanne, Switzerland). The detection limit of the GC method was ~3 ppm.

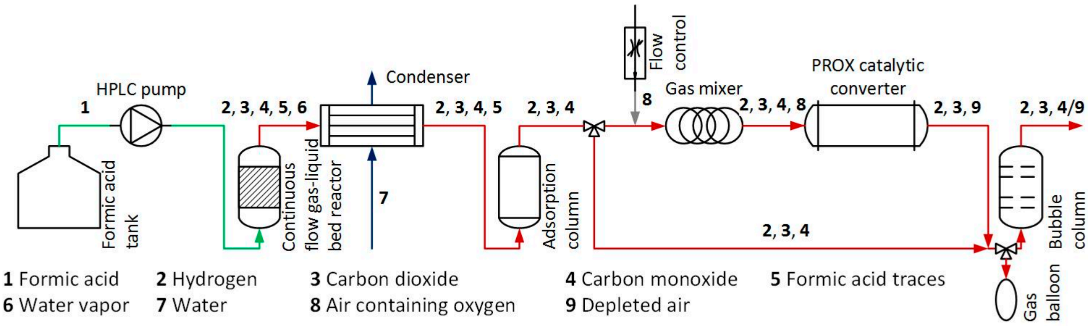

Figure 5. Scheme of the setup.

4. Conclusions

1. It was found that unwanted CO concentrations in $H_2 + CO_2$ gas streams catalytically produced through FA dehydrogenation over a homogeneous Ru-*m*TPPTS catalyst in a continuous-flow gas–liquid bed reactor (60–80 °C) was too high (8–70 ppm) to be used directly in a fuel cell. The CO concentration was dependent on the FA feed flow rate and reaction design (mixing).
2. It was shown that the Pt/Al_2O_3 catalyst can be easily implemented to clean $H_2 + CO_2$ gas streams from CO by PROX. It was shown that the O_2 supply should be fine-tuned well to prevent both a water clogging of the PROX catalyst and a H_2 loss due to its oxidation. Experimentally, CO concentration was confidently decreased by PROX at O_2 concentrations close to stoichiometry (0.008–0.065 v % O_2) to the level acceptable for fuel cell applications (<5 ppm). To our knowledge, this is the first example of successful CO removal from a FA reformate by PROX.

Acknowledgments: École Polytechnique Fédérale de Lausanne (EPFL), Swiss Competence Center for Energy Research (SCCER), Swiss Commission for Technology and Innovation (CTI) and Swiss National Science Foundation (SNSF) are thanked for financial support.

Author Contributions: G.L., I.Y. and V.H. conceived and designed the experiments; V.H. performed the measurements; N.A. and G.L. discussed the results, V.H., I.Y. and G.L. analyzed the data; V.H., I.Y. and G.L. wrote the paper.

Conflicts of Interest: The authors declare no conflict of interest.

References

1. Zhu, Q.-L.; Xu, Q. Liquid Organic and Inorganic Chemical Hydrides for High-Capacity Hydrogen Storage. *Energy Environ. Sci.* **2015**, *8*, 478–512. [CrossRef]
2. Dalebrook, A.F.; Gan, W.; Grasemann, M.; Moret, S.; Laurenczy, G. Hydrogen Storage: Beyond Conventional Methods. *Chem. Commun.* **2013**, *49*, 8735–8751. [CrossRef] [PubMed]
3. Sordakis, K.; Tang, C.; Vogt, L.K.; Junge, H.; Dyson, P.J.; Beller, M.; Laurenczy, G. Homogeneous Catalysis for Sustainable Hydrogen Storage in Formic Acid and Alcohols. *Chem. Rev.* **2017**. [CrossRef] [PubMed]
4. Moret, S.; Dyson, P.J.; Laurenczy, G. Direct Synthesis of Formic Acid from Carbon Dioxide by Hydrogenation in Acidic Media. *Nat. Commun.* **2014**, *5*, 4017. [CrossRef] [PubMed]
5. Eppinger, J.; Huang, K.-W. Formic Acid as a Hydrogen Energy Carrier. *ACS Energy Lett.* **2017**, *2*, 188–195. [CrossRef]
6. Li, Z.; Xu, Q. Metal-Nanoparticle-Catalyzed Hydrogen Generation from Formic Acid. *Acc. Chem. Res.* **2017**, *50*, 1449–1458. [CrossRef] [PubMed]
7. Fellay, C.; Dyson, P.J.; Laurenczy, G. A viable hydrogen-storage system based on selective formic acid decomposition with a ruthenium catalyst. *Angew. Chem. Int. Ed.* **2008**, *47*, 3966–3968. [CrossRef] [PubMed]
8. Boddien, A.; Mellmann, D.; Gärtner, F.; Jackstell, R.; Junge, H.; Dyson, P.J.; Laurenczy, G.; Ludwig, R.; Beller, M. Efficient Dehydrogenation of Formic Acid Using an Iron Catalyst. *Science* **2011**, *333*, 1733–1736. [CrossRef] [PubMed]
9. Himeda, Y.; Miyazawa, S.; Hirose, T. Interconversion between Formic Acid and H_2/CO_2 Using Rhodium and Ruthenium Catalysts for CO_2 Fixation and H_2 Storage. *ChemSusChem* **2011**, *4*, 487–493. [CrossRef] [PubMed]
10. Hull, J.F.; Himeda, Y.; Wang, W.-H.; Hashiguchi, B.; Periana, R.; Szalda, D.J.; Muckerman, J.T.; Fujita, E. Reversible Hydrogen Storage Using CO_2 and a Proton-Switchable Iridium Catalyst in Aqueous Media under Mild Temperatures and Pressures. *Nat. Chem.* **2012**, *4*, 383–388. [CrossRef] [PubMed]
11. Gan, W.; Dyson, P.J.; Laurenczy, G. Heterogeneous silica-supported ruthenium phosphine catalysts for selective formic acid decomposition. *ChemCatChem* **2013**, *5*, 3124–3130. [CrossRef]
12. Sharaf, O.Z.; Orhan, M.F. An overview of fuel cell technology: Fundamentals and applications. *Renew. Sustain. Energy Rev.* **2014**, *32*, 810–853. [CrossRef]
13. Baschuk, J.J.; Li, X. Modelling CO poisoning and O_2 bleeding in a PEM fuel cell anode. *Int. J. Energy Res.* **2003**, *27*, 1095–1116. [CrossRef]
14. Bröll, D.; Kaul, C.; Krämer, A.; Krammer, P.; Richter, T.; Jung, M.; Vogel, H.; Zehner, P. Chemistry in Supercritical Water. *Angew. Chem. Int. Ed. Engl.* **1999**, *38*, 2998–3014. [CrossRef]
15. Wakai, C.; Yoshida, K.; Tsujino, Y.; Matubayasi, N.; Nakahara, M. Effect of Concentration, Acid, Temperature, and Metal on Competitive Reaction Pathways for Decarbonylation and Decarboxylation of Formic Acid in Hot Water. *Chem. Lett.* **2004**, *33*, 572–573. [CrossRef]
16. Bjerre, A.B.; Sorensen, E. Thermal Decomposition of Dilute Aquaous Formic Acid Solutions. *Ind. Eng. Chem. Res.* **1992**, *31*, 1574–1577. [CrossRef]
17. Akiya, N.; Savage, P.E. Role of water in formic acid decomposition. *AIChE J.* **1998**, *44*, 405–415. [CrossRef]
18. Koper, M.T.M.; Shubina, T.E.; Van Santen, R.A. Periodic Density Functional Study of CO and OH Adsorption on Pt–Ru Alloy Surfaces: Implications for CO Tolerant Fuel Cell Catalysts. *J. Phys. Chem. B* **2002**, *106*, 686–692. [CrossRef]
19. Yano, H.; Ono, C.; Shiroishi, H.; Okada, T. New CO tolerant electro-catalysts exceeding Pt–Ru for the anode of fuel cells. *Chem. Commun.* **2005**, 1212–1214. [CrossRef] [PubMed]
20. Sung, L.Y.; Hwang, B.J.; Hsueh, K.L.; Tsau, F.H. Effects of anode air bleeding on the performance of CO-poisoned proton-exchange membrane fuel cells. *J. Power Sources* **2010**, *195*, 1630–1639. [CrossRef]
21. Sung, L.-Y.; Hwang, B.-J.; Hsueh, K.-L.; Su, W.-N.; Yang, C.-C. Comprehensive study of an air bleeding technique on the performance of a proton-exchange membrane fuel cell subjected to CO poisoning. *J. Power Sources* **2013**, *242*, 264–272. [CrossRef]
22. Schmittinger, W.; Vahidi, A. A review of the main parameters influencing long-term performance and durability of PEM fuel cells. *J. Power Sources* **2008**, *180*, 1–14. [CrossRef]

23. Mariño, F.; Descorme, C.; Duprez, D. Noble metal catalysts for the preferential oxidation of carbon monoxide in the presence of hydrogen (PROX). *Appl. Catal. B Environ.* **2004**, *54*, 59–66. [CrossRef]
24. Bion, N.; Epron, F.; Moreno, M.; Mariño, F.; Duprez, D. Preferential oxidation of carbon monoxide in the presence of hydrogen (PROX) over noble metals and transition metal oxides: Advantages and drawbacks. *Top. Catal.* **2008**, *51*, 76–88. [CrossRef]
25. Formanski, V.; Kalk, T.; Roes, J. Compact hydrogen production systems for solid polymer fuel cells. *J. Power Sources* **1998**, *71*, 199–207.
26. Panagiotopoulou, P.; Kondarides, D.I.; Verykios, X.E. Selective methanation of CO over supported noble metal catalysts: Effects of the nature of the metallic phase on catalytic performance. *Appl. Catal. A Gen.* **2008**, *344*, 45–54. [CrossRef]
27. Fellay, C.; Yan, N.; Dyson, P.J.; Laurenczy, G. Selective formic acid decomposition for high-pressure hydrogen generation: A mechanistic study. *Chem. Eur. J.* **2009**, *15*, 3752–3760. [CrossRef] [PubMed]